Analysis of Multiaxial Loading of Threaded Fasteners

Ernesto Camarena[1], Anthony Quintana[2], and Victoria Yim[3]

1.) *Purdue University* 2.) *New Mexico State University* 3.) *University of California, Berkeley*

Peter Grimmer[4], John Mersch[4], Jeff Smith[4], John Emery[4], Gustavo Castelluccio[5]

4.) *Sandia National Laboratories* 5.) *Cranfield University*

The simulation of various structural systems often requires accounting for the fasteners holding the distinct parts together. When fasteners are not expected to yield, simple reduced representations like linear springs can be used. However, in analyses of abnormal environments where fastener failure must be accounted for, fasteners are often represented with more detail. One common approach is to mesh the head and the shank of the fastener as smooth cylinders, neglecting the threads (referred to as a plug model). The plug can elicit a nonlinear mechanical response by using an elasto-plastic material model, which can be calibrated to experimental load-displacement curves, typically in pure tension. Fasteners rarely fail exclusively in pure tension so the study presented here considers current plug modeling practice at multiaxial loadings. Comparisons of this plug model are made to experimental data as well as a higher fidelity model that includes the threads of the fastener. For both models, a multilinear elastic-plastic constitutive model is used, and two different failure models are explored to capture the ultimate failure of the fastener. The load-displacement curves of all three sets of data (the plug model, threaded model, and the experiments) are compared. The comparisons between simulations and experiments contribute to understanding the role of multiaxial loading on fastener response, and motivate future work on improving fastener models that can accurately capture multiaxial failure.

I.   Nomenclature

CCOS	=	Critical crack opening strain
CTP	=	Critical tearing parameter
MLEP	=	Multilinear elastic-plastic
P	=	Reaction force magnitude
$P_{\bar{u}}$	=	Reaction force component in the direction of applied displacement
t_p	=	Tearing parameter
ε_p	=	Equivalent plastic strain
σ_{max}	=	Maximum principal stress
σ_m	=	Mean stress
θ_P	=	Angle of applied loading
θ_u	=	Angle of applied displacement

II.   Introduction

Hierarchical finite element analyses of complex systems are increasingly being used to inform design. Simulations are more economical than full scale experiments, especially for studying abnormal environments involving failure of various components within the system; sometimes it is simply impossible to test a system in certain abnormal conditions. Thus, the accuracy of simulations involving component failure is of crucial importance if a structure is to be designed to specific criteria when undergoing abnormal environments beyond the intended use of the system. Complex engineering structures contain joints between components, and these joints are often held together by threaded fasteners. The mechanical response of the system model depends on various length scales that span from the size of the components; to the size of the individual fasteners; to the size of the threads of the fastener. It is not generally possible to resolve the response of each individual fastener. However, the failure of joints typically depends

on the failure of individual fasteners, and as fasteners fail, the load paths within a structure can be dramatically altered. If joint failure is to be properly simulated in a large model, accurate surrogate models of the fastener must be used. These surrogate models range in fidelity from a simple spot-weld [1] (a user-specified nonlinear load-displacement relationship constraining the two parts together) to more physics-based models like a meshed "plug" of elements with element plasticity and failure [1], [2].

The current typical method of generating a nonlinear fastener model is to pick a simplified geometric model form, and then calibrate its response to correspond to a given fastener. In the absence of rich test data on a given fastener, information from a fastener spec sheet or standard can be used to estimate reasonable constitutive parameters for the fastener model. For example, SAE J429 [3] provides yield stress, ultimate stress, and elongation-to-failure specification minimums that can be used to parametrize a fastener model. Calibrating to specifications is assumed to be less accurate but more conservative than calibrating to test data. When the full load-displacement response of a given fastener is available from experiments, then the fastener model can be calibrated to the test data via an inverse finite element analysis approach [4]–[6].

The data used to calibrate a fastener model (from a specification or testing) is usually specific to the fastener's response in tension. However, fasteners can experience general combined loading in service. Models calibrated to tension are commonly relied upon to predict fastener response to general loading, the implications of which remain unknown. There have been several efforts to experimentally characterize the response of fasteners at different angles of applied loading; this work utilizes data from multiaxial fastener tests performed at Sandia National Labs, and NASA carried out a similar test program [7]. These studies utilized novel test fixtures that allow for fasteners to be loaded at various angles of combined tensile-shear loading using a standard tension test machine (Fig. 1). In this work, multiaxial fastener tests are simulated, using two different fastener models, to evaluate how well the models can capture the response of the fastener at the various test angles. We find that the overall qualitative trends of the test can be captured by the models, but we failed to demonstrate that a given fastener model can use one constitutive model to accurately predict all of the test angles. This suggests that fastener reduced order models must be further developed to be able to accurately capture the response to general loading.

III.   Methodology

In 2012, quasi-static tests of combined tensile-shear loading were performed on No. 4 (.25" outer diameter) UNF thread type [8] stainless steel 18-8 fasteners (McMaster-Carr part #92196A317) at Sandia National Labs. For this work, data is analyzed from four angles of loading; namely 0°, 30°, 60°, and 90°. The angles are given relative to the screw axis, so 0° corresponds to pure tension and 90° corresponds to pure shear. Several tests were conducted for each load angle, but for this study a single representative load-displacement curve from each test was used. Load-displacement data from these tests were used for comparisons to the FE models presented herein. Fig. 1 illustrates a portion of the test setup and a detail view of how the fastener holds the two bushings together.

A total of three FE models were used during this study. Initially a plug model without bushings (hereafter referred to as "basic plug") was used to calibrate the constitutive model to the 0° experimental data. A multi-linear elastic-plastic (MLEP) constitutive model was used to define how the yield surface evolves with increasing plastic strain. The basic plug was repeatedly ran and the hardening curve and failure model parameters were modified until the model load-displacement results agreed with the experiment (an inverse procedure [4]–[6]). The remaining two models represented the steel bushings to more accurately resolve the boundary conditions that the tests applied to the fasteners. The calibrated MLEP constitutive model was then input into both a plug model and threaded model with bushings (hereafter referred to as "plug model" and "threaded model" respectively). The ultimate failure of the plug and threaded model were initially controlled with a simple element death damage model consisting of a loss of element stiffness after a critical plastic strain. Then, a phenomenological ductile damage model [9] was incorporated. The constitutive parameters that were adjusted for calibration are the MLEP hardening curve points, and the damage model parameters. These parameters were calibrated on the plug model and then used in the threaded model for comparisons. All models used uniform gradient, 8-node hexahedral elements and were simulated using Sierra/SM [10].
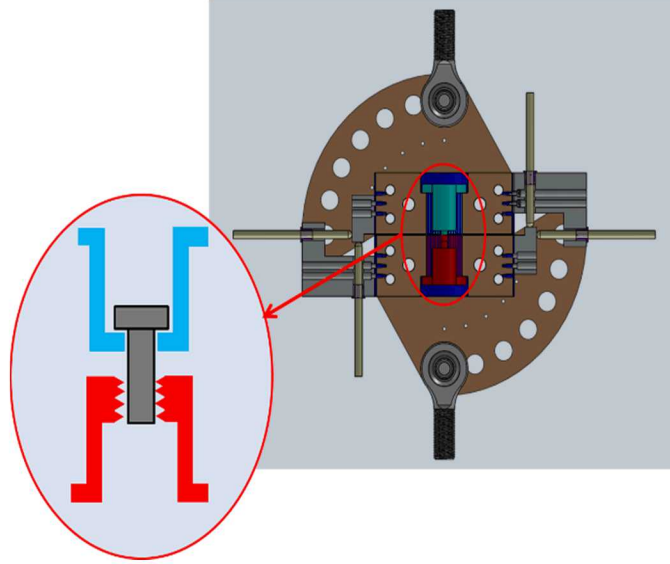
Figure 1: Multiaxial fastener test setup. This setup allows for loading the fasteners at various angles from 0° to 90°.

A. Geometry

The low-fidelity plug model has a relatively simple geometry, consisting of two smooth cylindrical sections representing the head and the shank. The cross-sectional area of the shank was modeled after the tensile stress area of the real fastener [8]. The smooth shank of the plug is held into the mating base material with tied contact.
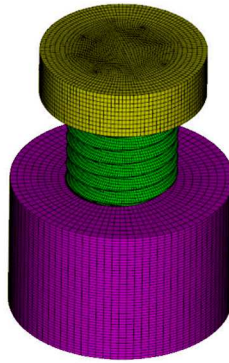

Figure 2: Threaded model geometry embedded in nut.

The high-fidelity threaded model (Fig. 2) better resolves the fastener geometry and was created by sweeping cross sections of the fastener helically along the fastener's vertical axis [11]. A nut for the threaded model was built and meshed in a similar way, represented in purple in Fig. 2. Frictional contact was used between the nut and the shank threads, with a coefficient of friction of 0.30. Previous work has suggested that the results should be relatively insensitive to the coefficient of friction [2]. The nut was then embedded in the bushing geometry using tied contact.

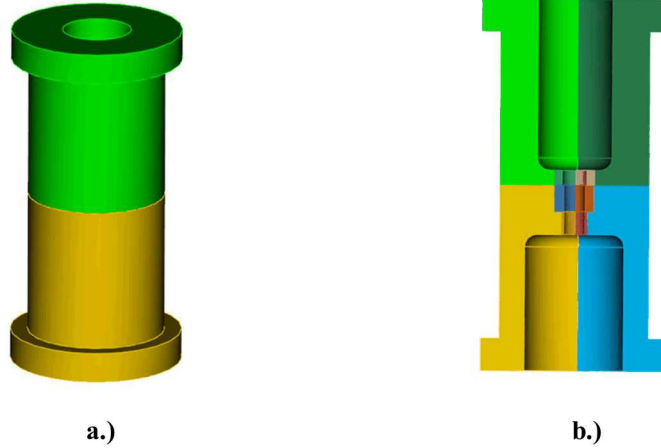a.)   b.)

Figure 3: Bushings. a.) Outside of bushings. b.) Cross section of bushings (colored according to geometry decompositions performed to facilitate hex meshing)

Both models are embedded in the same bushings as illustrated in Figure 3; although the regions that interface with the shanks of each model are slightly different to accommodate their respective geometries. The bushings are meshed coarser than the plug and threaded models. The mesh in the regions near the fastener are refined, illustrated in Fig. 4. Tied constraints were used between the plug and the region in the bushings on the bottom portion of the shank, shown in red in Fig. 4a.
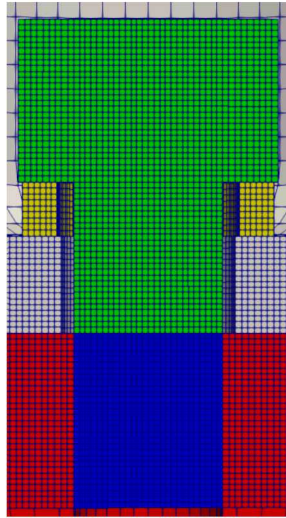

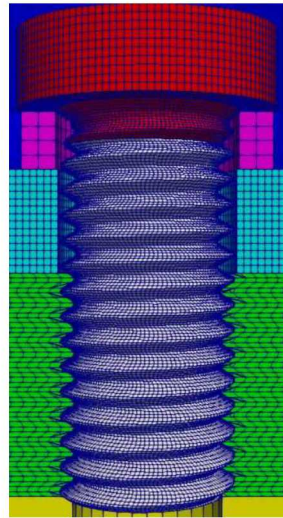**Figure 4a: low-fidelity plug model with refined bushings**

Figure 4b: high-fidelity threaded model with refined bushings

B. Boundary Conditions

To achieve applied load displacement corresponding to the desire angles of loading, certain node sets of the mesh were selected. Based on these selected node sets, either a prescribed displacement was applied to the upper bushings, or zero displacement was used to constrain desired directional motion. The basic plug was only tested in the 0° case (pure tensile loading) for the calibration of the hardening curve. As depicted in Fig. 5a, the node set located under the plug head was prescribed a $+z$ displacement, fixed in the z-direction on the lower node set. The 'Plug Model' and 'Threaded Model', however, required more careful boundary conditions to achieve the desire angle of displacement to match our experimental data. As illustrated in Figs. 5b and 5c below, for the cases of 30° and 60°, the upper bushing is prescribed a combination of shear and tensile displacements according to the correct angular displacement. For example, in the 30° case, a $+z$ displacement is given to the lower face node set of the upper bushing, while

simultaneously a $-x$ displacement was applied over the $+x$ node set of the upper bushing. In all cases, an opposite fixed displacement was used to ensure symmetry across all prescribed displacement angles.
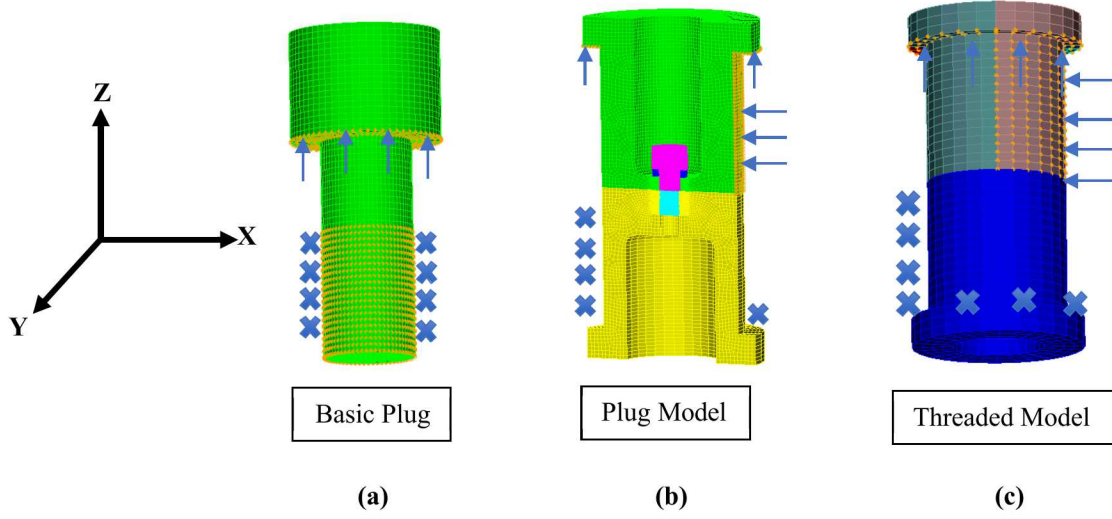

Figure 5: Boundary conditions. a) Basic Plug, b) Plug Model (with bushings) c) Threaded Model

It was necessary to consider the misalignment between the load pull direction and reaction force line of action. Fig. 6 illustrates the difference between the direction of the applied displacement, the reaction force, and their respective angles θ_u and θ_P. It was determined that for comparisons to the experiments, the projection of the reaction force in the direction of the applied displacement should be used, rather than the total magnitude of reaction force on the bushings, as this has some component perpendicular to the frame of the loading machine from the test. This introduces a model form error, as the true tests did not produce reaction loads perpendicular to the axis of the machine. This indicates that the displacements experienced by the fastener in the tests likely do not correspond exactly to the nominal angles of the load fixture. This is an unknown source of uncertainty in the comparison between analyses and experiment, and thus the main goal of this work is simply to capture general trends as the loading changes from tensile to shear. The projected load was computed with Eq. 1 for the 30° and 60° cases.

$$P_{\bar{u}} = P \cos(\theta_u - \theta_P) \tag{1}$$

where

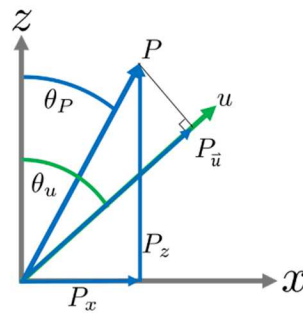$$\theta_P = \tan^{-1}\left(\frac{P_x}{P_z}\right) \tag{2}$$

Figure 6: Misalignment between reaction force and pull direction.

IV. Results

A. Load-Displacement Comparisons

Fig. 7 compares the plug model, the threaded model, and the experiments at each pull angle (0°, 30°, 60°, and 90°). The insets to the figure show contours of Von Mises stress for the plug model, just prior to the onset of failure. The plug and threaded models show similar load-displacement responses and they both capture the overall behavior of the experimental data, except for the 90° case. The boundary conditions applied to the 90° case cause highly localized deformations that may not be present in the real test; this issue is later explored in Results Section C. The failure model utilized in Fig. 7 was element death based on a critical value of equivalent plastic strain, ε_p, which was calibrated to the 0° (tension) test. This failure model provides a reasonably accurate displacement-to-failure (as seen by a reduction in load) for the 30° case, but cannot accurately be extended to 60° and 90°. This suggests that a more accurate failure model must be used for accurately predicting displacement-to-failure in general loading.

It was interesting to track the angle of applied loading, θ_P, through the range of displacements as shown in Fig. 8. The 30° and 60° case are plotted as well as the 0° case as a reference. As expected, the 0° case has $\theta_P = \theta_u$. However, the 30° and 60° case both show that θ_P is less than θ_u. This indicates that our comparisons to the 30° and 60° tests may not be directly comparing the same loading angle; however, the trends as the angle increases can still be analyzed.
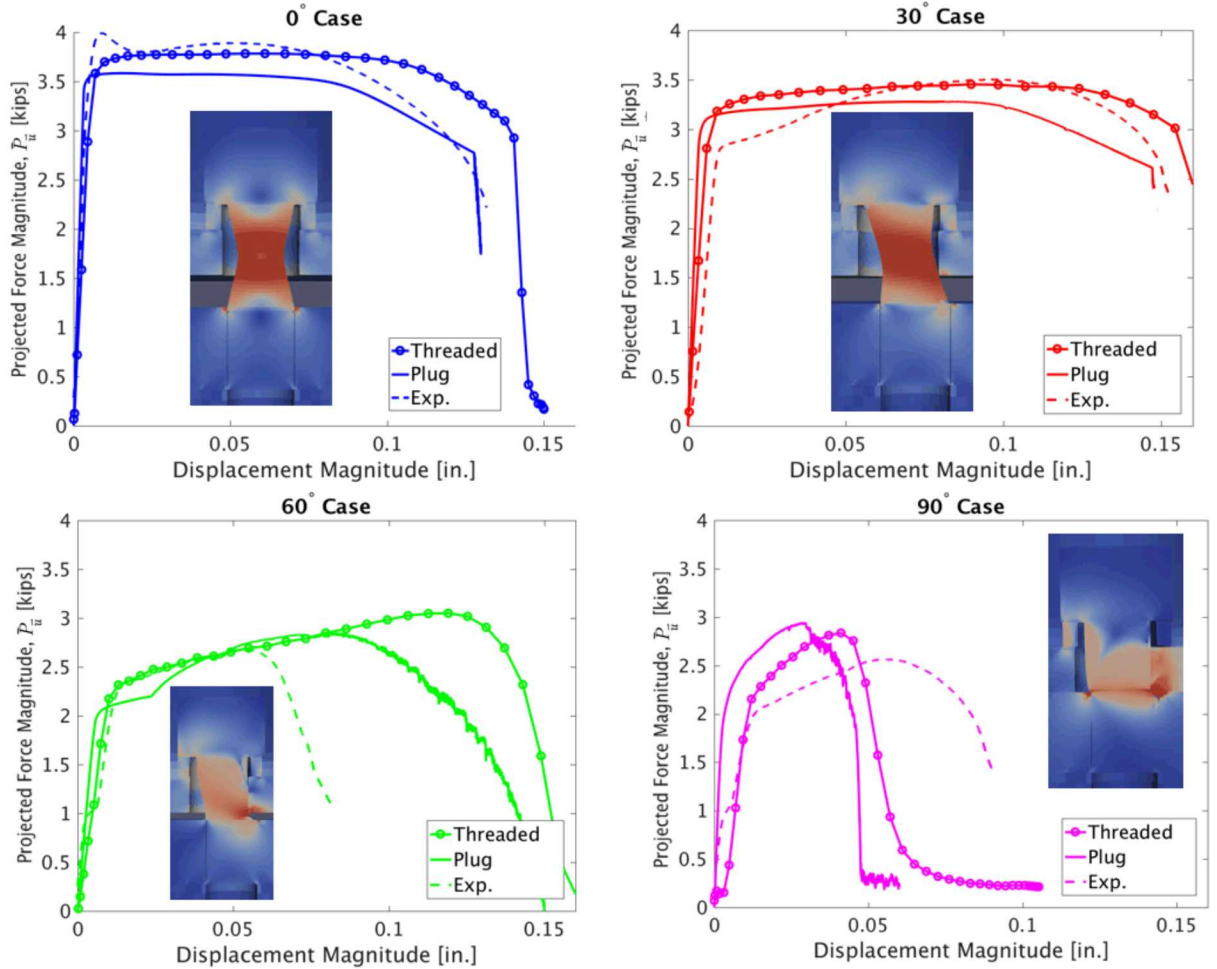

Figure 7: Comparison of the plug and threaded model verses experimental data for various angles. The contour plots are Von Mises stress for the plug model.
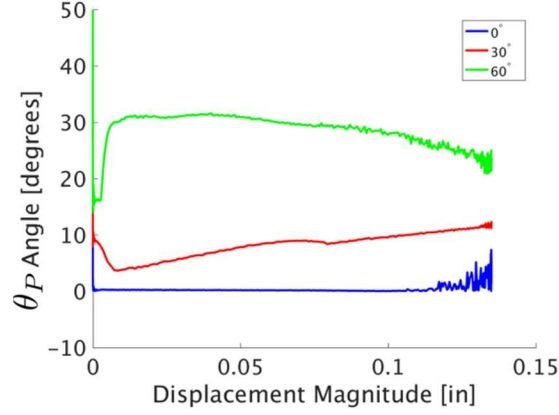
Figure 8: Variation of the angle of applied loading with displacement magnitude.

B. Ductile Damage Failure model

This study considered several failure models to represent the ultimate failure of the tests (observed by the reduction in load corresponding to the fastener breaking). The initial failure model used was simply to delete elements (e.g. instantaneously assign them zero stiffness) when they reached a critical value of equivalent plastic strain. We found that this crude failure model could not be accurately extended to other angles once calibrated to a specific angle. Thus, to attempt to better predict failure at all the test angles a more sophisticated ductile damage model [9] was used. This failure model utilizes two derived state variables, the tearing parameter (t_p) and the crack opening strain (*COS*), to define how a given element's stiffness is reduced as it accumulates damage. The tearing parameter is computed for a given element according to Eq. 3:

$$t_p = \int_0^{\varepsilon_p} \left[\frac{2\sigma_{max}}{3(\sigma_{max}-\sigma_m)} \right]^m d\varepsilon_p \tag{3}$$

where σ_{max} and σ_m are the maximum principal and mean stresses, respectively, ε_p is the equivalent plastic strain, and *m* is a user-defined parameter with a default value of 4. Due to the dependence of Eq. 3 on the mean stress, σ_m, increasing the value of *m* amplifies the triaxiality dependence of the tearing parameter. In this study, *m* was left as its default value of 4. The tearing parameter defined by Eq. 3 controls when damage initiates; then, once *CTP* is reached, how quickly the element's stiffness is reduced is controlled by the crack opening strain, *COS*. The crack opening strain is defined as the additional strain in the direction of the max principal stress from the step in which *CTP* was first reached. The stiffness of the element will then linearly decrease from its current value to zero as crack opening strain increases from zero to the user-defined critical crack opening strain, *CCOS*. The value of *CCOS* effectively defines how much energy a given element dissipates as it fails. Once *CTP* is reached the ductile damage model takes over from the overall constitutive model defining prior element plasticity. Thus, this is an uncoupled damage model which has no influence on the element until damage initiates at *CTP*. It should be noted that the tearing parameter reduces to the equivalent plastic strain for uniaxial tension, but deviates from it for other stress states.

To calibrate our models, several critical tearing parameters (*CTP*) and critical crack opening strain (*CCOS*) values were considered to best match the experimental data. The 60° plug model was used to calibrate *CTP* and *CCOS* (Fig. 8). These values were then applied to both models for all angles of displacement (Fig. 9).
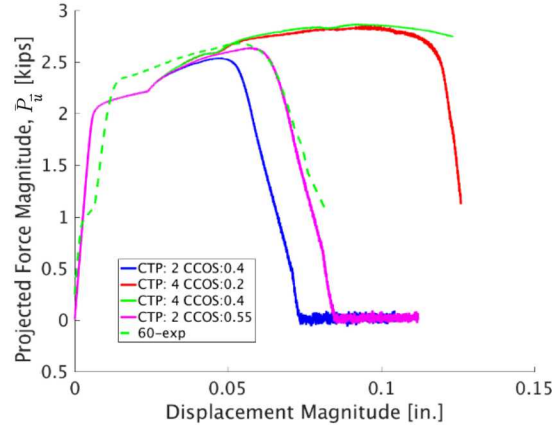
Figure 9: Load-Displacement: varying *CTP* and *CCOS*

The final results of this study indicated the best result for the plug model at 60° was a *CTP* value of 2, and a *CCOS* value of 0.55. These values were then used for both the plug, and threaded models at all angles (Fig. 9).
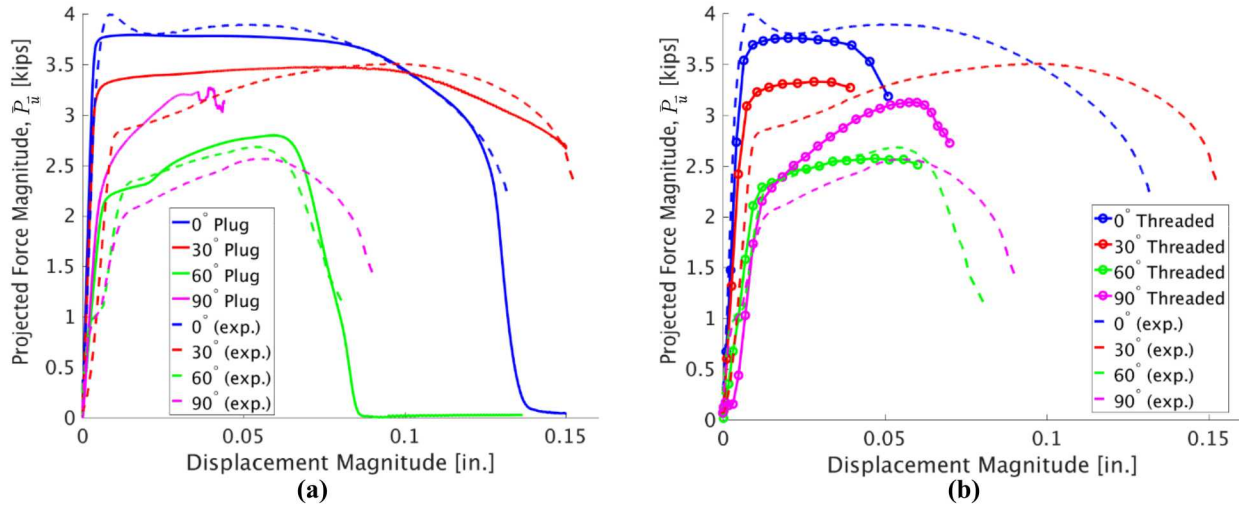

Figure 10: Load-displacement: (a) plug with bushings to experiments (b) threaded models to experiments

The plug model calibrated to 60° also did reasonably well at predicting the failure displacements of the 0° and 30° cases. The 90° case still has the model form issues that prevented it from doing well before using this failure model. When using the *CTP* and *CCOS* values calibrated to the plug on the threaded model, failure is seen at lower displacements. This is expected, as the threaded model has amplified stresses due to its geometry, and the tearing parameter and crack opening strain depend on the stress state. Furthermore, *CCOS* is naturally element size dependent, and the threaded model has smaller elements than the plug model. There was insufficient time to separately calibrate *CTP* and *CCOS* to the threaded model, but that would be an interested avenue for future work.

C. Bushing Gap Study

The 90° simulations did not agree well with the experiments for any of the models. The boundary conditions used for the pure shear case tend to create highly localized deformation. Thus, for the 90° case, it was sought to spread the deformation by incorporating a gap between the two bushings. The gap sizes used were 0.02, 0.04, and 0.06 inches. The results, shown in Fig. 11, showed that increasing the distance between the two bushings also increased the displacement at which the plug model failed, and reduced the max load. A gap of 0.04 inches best matched the failure

displacement from the experimental data, although the force at which it yielded was still higher than that of the experiment.
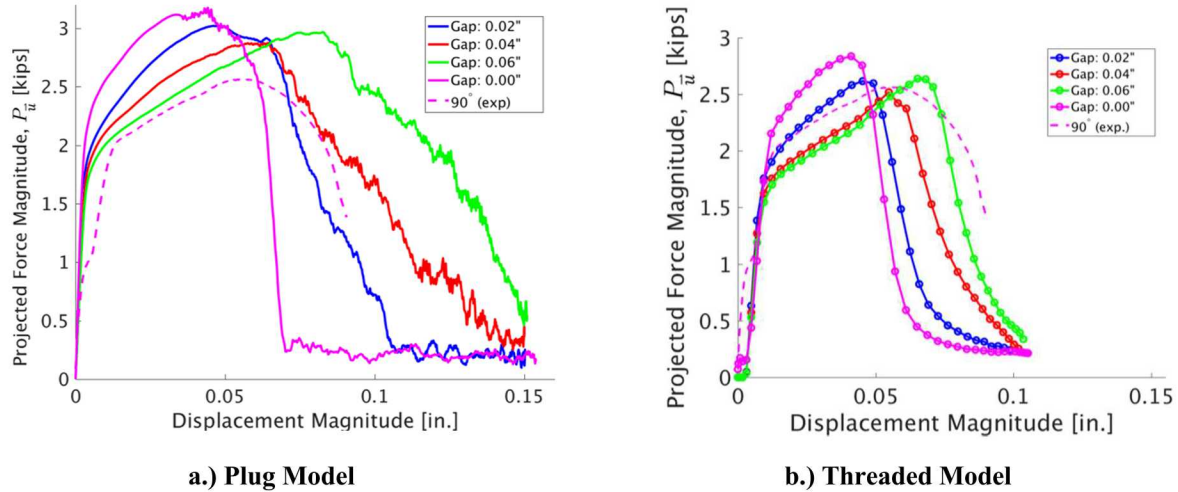

a.) Plug Model　　　　　**b.) Threaded Model**

Figure 11: Load-displacement of 90° case with varying gap size between bushings compared against experiment

A similar trend was observed for the threaded model when giving it a gap between the two bushings (Fig. 11). These results suggest that it's possible that during the shear experiments, the bushings gapped, and the fastener experienced some bending rather than the highly localized shearing seen in the models with no gap.

V.　　Conclusions

Finite element models of fasteners subjected to combined tensile-shear loading at various angles were compared to analogous experiments on stainless steel 18-8 0.25" UNF fasteners (McMaster-Carr part #92196A317). Two different models were used to represent the fastener; a smooth plug model, and a fully 3D helical threaded model. The models could capture the load-displacement response of the 0° and 30° tests, but did not do as well at matching the 60° and 90° tests. The plug model's predictions of displacement-to-failure were mildly improved when switching from a crude damage model based strictly on plastic strain to a more refined ductile damage model [9]. The plug model and the threaded model gave qualitatively similar load-displacement responses prior to damage initiation. There was insufficient time to calibrate the ductile damage model to the threaded model for this work, but that would be a potential way to improve predictions of displacement-to-failure, as the more accurate geometrical representation elicits a more realistic stress state than the plug model. Overall, this work demonstrated that high fidelity models of fasteners that incorporate plasticity can capture experimentally measured trends in multiaxial loading of fasteners, but care must be taken in the application of boundary conditions if direct test-analysis comparisons are to be made.

==Potential additional things to write about if we want to have a full Discussion section (do we want/need to?):==

- Load vs displacement response
  - Note that the angles displaced in these simulations do not necessarily correspond to the angles experienced by the fastener in the tests
    - In the tests there wasn't actually any transverse reaction forces, the fixtures rotated to alleviate this.

- - o Plug does alright in 0 and 30, not great in 60 and 90
    - o Plug and threaded are fairly similar prior to failure models kicking in
    - o Believe there is a model form error in 90
      - ▪ Boundary conditions do not perfectly match the test
      - ▪ Adding gap helped improve agreement. Possible that the bushings pull apart as they're sheared
  - Failure models
    - o Eqps death does a bad job when extended away from tension for both plug and threaded
      - ▪ It's not just the model form of the plug being wrong, this failure model is just too crude.
    - o Calibrated ductile damage model to plug
      - ▪ This improved general agreement across all angles other than 90, which has a known model form error.
      - ▪ Ductile damage model is probably too strong in shear, as tearing parameter increases at a faster rate with high triaxiality and our shear BC's lead to low triaxiality.
      - ▪ Failure model calibrated to the plug was way off for the threaded model.
        - • Did not have time to calibrate to the threaded model, but showed that the ductile damage parameters calibrated to the plug are not indicative of the fastener material since increasing geometric fidelity caused different results.
  - Future directions
    - o Investigate use of more accurate failure models that treat tensile and shear stress states separately
      - ▪ e.g. BCJ model
    - o Calibrate damage models to the threaded model
      - ▪ Higher geometric fidelity means constitutive model is more indicative of material properties, and thus this model could be more accurately extended outside of tested regimes
        - • Use to generate virtual test data for untested fasteners.

Acknowledgments

References

[1] J. P. Mersch, J. A. Smith, and E. P. Johnson, "A Case Study for the Low Fidelity Modeling of Threaded Fasteners Subject to Tensile Loadings at Low and High Strain Rates," p. V002T02A020, Jul. 2017.

[2] G. M. Castelluccio and M. R. W. Brake, "On the origin of computational model sensitivity, error, and uncertainty in threaded fasteners," *Comput. Struct.*, vol. 186, pp. 1–10, 2017.

[3] "SAE J429: Mechanical and Material Requirements for Externally Threaded Fasteners." SAE, Apr-2013.

[4] A. Husain, D. K. Sehgal, and R. K. Pandey, "An inverse finite element procedure for the determination of constitutive tensile behavior of materials using miniature specimen," *Comput. Mater. Sci.*, vol. 31, no. 1, pp. 84–92, Sep. 2004.

[5] J. M. Emery, R. V. Field Jr, J. W. Foulk III, K. N. Karlson, and M. D. Grigoriu, "Predicting laser weld reliability with stochastic reduced-order models," *Int. J. Numer. Methods Eng.*, vol. 103, no. 12, pp. 914–936, 2015.

[6] J.-C. Gelin and O. Ghouati, "An inverse solution procedure for material parameters identification in large plastic deformations," *Commun. Numer. Methods Eng.*, vol. 12, no. 3, pp. 161–173, Mar. 1996.

[7] B. E. W. Steeve, "Aerospace Threaded Fastener Strength in Combined Shear and Tension Loading," Mar. 2012.

[8] "ASME - STANDARDS - Unified Inch Screw Threads, (UN and UNR Thread Form)." [Online]. Available: https://www.asme.org/products/codes-standards/unified-inch-screw-threads--un-and-unr-thread-form. [Accessed: 11-Jun-2018].

[9] G. Wellman, "A simple approach to modeling ductile fracture," Sandia National Laboratory, Albuquerque, NM, Sandia Report SAND2012-1343, 2012.

[10] S. Solid Mechanics Team, "Sierra/Solid Mechanics 4.48 User's Guide," Sandia National Laboratory, Unlimited Release SAND202018-2961, Mar. 2018.

[11] T. Fukuoka and M. Nomura, "Proposition of Helical Thread Modeling With Accurate Geometry and Finite Element Analysis," *J. Press. Vessel Technol.*, vol. 130, no. 1, pp. 011204-011204–6, Jan. 2008.